



Influence of the Addition of Two Transition Metal Ions to Sodium Zinc Borophosphate Glasses for Optical Applications

A. M. El-Batal^a, M. A. Farag^{b*}, M. M. El-Okr^b, Aly Saeed^c

^aPhysics Department, Al-Safwa Higher Institute of Engineering and Technology, Cairo, Egypt.

^bPhysics Department, Faculty of Science, Al-Azhar University, Cairo, Egypt.

^cMathematical and Natural Sciences Department, Faculty of Engineering, Egyptian-Russian University, Cairo, Egypt.



CrossMark

Abstract

Effect of Co and Mo ions on the sodium zinc borophosphate glasses network was investigated. Both structural and optical properties were studied by X-ray diffraction, density, infrared spectroscopy and optical absorption. Only a broad halo was observed in the X-ray diffraction patterns indicating the non-crystalline nature of the prepared samples. Density and related parameters such as molar volume and average boron-boron separation showed that the glass network became more compact by increasing Mo oxide. Fourier Transform Infrared (FTIR) spectroscopy results showed that the free Co and Mo sample revealed the formation of structural building units of the borate and phosphate glasses. The addition of Co and Mo oxides cause variation in structural sites of the glass formers which appear as a small change in the FTIR spectra. The optical absorption spectra in the UV-Visible regions were used to study the optical d-d transitions of Co and Mo ions. Deconvolution of the absorption spectra gave multi-bands in the UV-Visible regions which, are related to the presence of various oxidation states of the two transition metal ions, cobalt and molybdenum, octahedral and tetrahedral of Co²⁺, octahedral of Co³⁺, Mo³⁺, and Mo⁵⁺. The calculated optical energy gap, Urbach energy and refractive index of all the prepared samples were found to be glass composition dependent.

Keywords: Transition metals, Borophosphate glasses, Structural and optical properties, Optical filters.

1. Introduction

Glass is one of the most important pillars in the modern technology, such as optical filters, optical fibers, dosimeters, smart windows, solid batteries and lasing mediums. In this regard, glasses have received great attention due to their several applications. [1-4]. Optical glass filters have a great technological interest, which come from their ability to transmit a certain band of wavelengths. Among the different types of optical filters, the band-pass filter has priority due to its ability to transmit a portion of the spectrum while blocking other wavelengths. Such optical filters are ideal for a variety of applications, such as fluorescence, spectroscopy, clinical chemistry, or imaging. Also, these filters are typically used in the life science, industrial, or R&D industries. [2-3].

Borophosphate glass is one of the important glasses, due to their peculiar properties and wide range of applications. Moreover, borophosphate glass are used in different technological aspects such fast ionic conductor, low-melting glass solder, glass-to-metal seals and bio-medical applications [4-5].

Recently, there has been enhanced interest in studying synthesis, structure and physical properties of transition metal oxide doped glasses due to their peculiar optical characteristics. The transition metal ions are incorporated into the glasses in order to improve and modify their optical, structural, magnetic and electronic properties [6]. In this respect, ZnO acts as a good glass modifier in the borophosphate glasses also it suppresses hydration reactions and reduce the residual stresses in the glass samples [7].

Doping glass materials with molybdenum affects their magnetic, optical, and electrical properties [8]. In such case polarons has considerable contribution to conductivity, due to the possible of two valence states Mo⁵⁺ and Mo⁶⁺ ions [9]. The latter gives such glasses its photochromic behavior. The doping with cobalt ions creates colour centres (blue, pink or red), its colour changes with the transformation of its tetrahedral coordination to octahedral for a change in melt composition with absorption bands in the visible and NIR regions. [10-11]. On the other hand, cobalt ion exists in mixed valence octahedral and tetrahedral sites which, make it a promising modifier for many applications such as solar selective absorbers, fuel cells, and visible and near-infrared laser materials [6-7].

*Corresponding author: moha_far.1@azhar.edu.eg; moha_far2010@yahoo.com

Received Date: 08 June 2021, Revised Date: 27 June 2021, Accepted Date: 30 June 2021

DOI: 10.21608/EJCHEM.2021.79765.3921

©2021 National Information and Documentation Center (NIDOC)

In this work we aimed to study the dependence of structural and optical properties of zinc sodium borophosphate glasses on Co and Mo addition. Sodium oxide was added to the prepared glass network to expand the glass-forming region and facilitate ion exchange and provide low melting glass. The studies include X-ray diffraction, density, FTIR, and optical absorption. In addition, some structural and optical parameters were calculated.

2. Experimental Procedure

A series of glasses samples with chemical composition $50 \text{ B}_2\text{O}_3 - 15 \text{ P}_2\text{O}_5 - 10 \text{ ZnO} - (25 - x) \text{ Na}_2\text{O} - x \text{ MoO}_3 - y \text{ CoO}$ where $x = 0, 0.2, 0.4, 0.6$ and 0.8 while $y = 0$ and $(1-x)$ were prepared using the conventional melt quenching method. The chemicals used are analytical grade. The starting materials are zinc oxide, boric acid, ammonium di-hydrogen phosphate, sodium carbonate, cobalt oxide and molybdenum oxide. The proper weights were mixed together continuously using a mortar and the mixture was melted in porcelain crucible at about 1100°C using electric furnace for about 1 h. The molten were shaken to get homogenize melt. Ingot glasses were subjected to anneal at 300°C for 2 h to avoid the residual stresses developed during the quenching process. The chemical composition of the prepared samples is shown in detail in **Table 1**.

Table 1: The chemical composition of the prepared samples

Sample No	Chemical Composition, mol%					
	B_2O_3	P_2O_5	ZnO	Na_2O	MoO_3	CoO
S0	50	15	10	25	0	0
S1	50	15	10	24	0	1
S2	50	15	10	24	0.2	0.8
S3	50	15	10	24	0.4	0.6
S4	50	15	10	24	0.6	0.4
S5	50	15	10	24	0.8	0.2

The XRD patterns of the prepared samples were used to check the structural state of the prepared samples. The density of the glasses prepared was determined by conventional Archimedes' method using Carbon tetrachloride (CCl_4) as the buoyant liquid. A Fourier Transform Infrared (FTIR) spectrometer, Perkin Elmer spectrometer, RTX, was used to study the local structural units. UV-VIS absorption spectra were obtained for highly polishing samples using spectrophotometer (type JASCO Crop., V-570, Rel-00, Japan) covering the wavelength range from 190 to 1100 nm.

3. Results and discussion

3.1. XRD

XRD patterns of the prepared samples are shown in **Figure 1**. No diffraction peaks, however only one broad halo was observed in the patterns at $2\theta \approx 27^\circ$ which indicate the glassy state of the prepared samples.

3.2. Density

The measured density (ρ) and the molar volume V_M of the studied glasses were estimated using the following equations [12-13]

$$\rho = \frac{W_a}{W_a - W_l} \times \rho_l$$

$$V_M = \frac{M}{\rho}$$

where; W_a and W_l is the sample weight in air and CCl_4 respectively, ρ_l is the density of CCl_4 , and M is the glass molecular weight in the mol%.

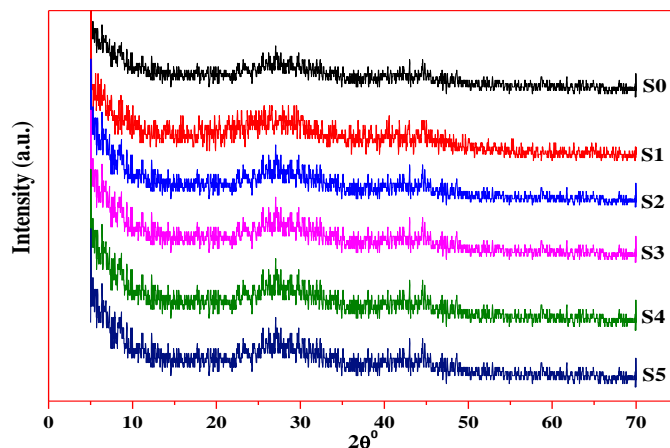


Fig 1: XRD profile of $\text{B}_2\text{O}_3 - \text{P}_2\text{O}_5 - \text{ZnO} - \text{Na}_2\text{O} : \text{MoO}_3 + \text{CoO}$ glass

The measured density and calculated molar volume are listed in **Table 2**. It is observed that the density increases with increasing MoO_3 content while the molar volume decreases. The observed increase in the density was attributed to the molar mass of the MoO_3 is heavier than the molar mass of the other constituents in the glass network. The decrease in molar volume confirms that the molybdenum increases the reticule of the network. The observed behaviour of density and molar volume indicates that the glass structure becomes more compact due to the presence of Mo ions in interstitial position of glass network [14].

The average boron-boron separation d_{B-B} was calculated to confirm the compactness of glasses due to the presence of MoO_3 according to the following relations [15]

$$d_{B-B} = \left(\frac{V_M^B}{N_A} \right)^{\frac{1}{3}}$$

$$V_M^B = \frac{V_M}{2(1 - X_B)}$$

where the volume V_M^B corresponds to the volume that contains one mole of boron within the given structure and X_B molar fraction of B_2O_3 . The obtained results of d_{B-B} are illustrated in **Table 2**.

The progressive decrease in the d_{B-B} with increase of MoO_3 confirm the homogeneity and increase of compactness of the glass network i.e. increase the prepared glass density.

The observed behaviour of density, molar volume, and average boron-boron separation showed that the addition of both Co and Mo cause a strong change in the glass network. In order to get more information about the influence of CoO & MoO_3 on the glass network, the ion concentration N_i (ions/ cm^3), polaron radius r_p (\AA), inter atomic distance r_i (\AA) and field strength F (cm^{-2}) around Co and Mo ions are calculated according to the following relations [16-17] and tabulated in **Table 2**.

$$N_i = \frac{x\rho N_A}{M_W}$$

$$r_i = \left(\frac{1}{N_i} \right)^{\frac{1}{3}}$$

Table 2: Structural and optical properties of the studied glass

Sample	S0	S1	S2	S3	S4	S5
Calc. parameters						
ρ (gm/cm ³)	2.443	2.454	2.513	2.525	2.534	2.54
V (cm ³ /mol)	32.632	32.547	31.829	31.734	31.682	31.655
d_{B-B} (°A)	3.783	3.780	3.753	3.748	3.746	3.745
d_{P-P} (°A)	3.170	3.167	3.144	3.141	3.139	3.139
$N_i \times 10^{22}$	0	1.847	3.778	5.684	7.589	9.497
r_i (°A)	0	3.783	2.98	2.601	2.362	2.192
r_p (°A)	0	1.524	1.201	1.048	0.952	0.883
$F \times 10^{15}$ cm ⁻²	0	3.494	5.629	7.391	8.967	10.041
n	2.215	2.203	2.350	2.472	3.010	2.492
$\alpha_0^2(n)$	2.785	2.761	2.890	3.021	3.494	3.036
$\Lambda_{Exp.}$	1.070	1.065	1.092	1.117	1.192	1.120
ϵ	4.905	4.851	5.523	6.110	9.062	6.210
M	0.434	0.438	0.399	0.370	0.271	0.365

$$r_p = \frac{1}{2} \left(\frac{\pi}{6N_i} \right)^{1/3}$$

$$F = \frac{Z}{r_i^2}$$

where N_A Avogadro's number, M_W molecular weight, Z oxidation number, and x is mol. % of modifiers.

It is observed in **Table 2** that the interatomic distances are greater than the polaron radius. In addition, both r_i and r_p decrease as the addition of Mo amount increases. This behaviour confirms that the molybdenum ions act, in the present glass system, as modifier and make the glass network to be more compact which in turn increases the density.

3.3. FTIR

The FTIR spectra registered for the studied glasses in the 400-1600 cm⁻¹ frequency range are shown in **Figure 2a**. The obtained FTIR spectra are deconvoluted using a Gaussian-type function as shown in **Figure 2b**. Because the studied glasses contain two different glass former oxides both network of phosphate groups, triangular and tetrahedral.

borate units are expected to appear in the FTIR spectra. In **Figure 2a**, three different wide bands are observed as following: i). Three clear absorption bands located at 532, 700, and 1527 cm⁻¹; ii). Two shoulders located at 1285 and 1403 cm⁻¹; iii). Very low intensity bands located at 987, 1095 and 1643 cm⁻¹. The observed band located at 532 cm⁻¹ can be assigned to the bending harmonic of O=P-O bands. The band at 700 cm⁻¹ corresponds to the bending vibrations of B-O-B

groups in various borate segments.

The band located at 987cm⁻¹ is usually attributed to bending vibration of P-O-P, symmetric stretching of $P_2O_7^{4-}$, and stretching vibration of BO_4 [18-19]. The bands at 1095 cm⁻¹ are characteristic of terminal P-O and PO_3 groups, and the sharing of stretching vibrations of tetrahedral BO_4 groups [20]. The absorption band at 1265 cm⁻¹ are characteristic to vibrations of non-bridging PO_2 groups, and also sharing the vibrations of BO_3 groups [20]. The absorption band located at 1527 cm⁻¹ and the shoulder at 1403 cm⁻¹ are attributed to the bending vibration and stretching vibration of B-O-B in $[BO_3]$ triangles [21]. The spectral band at 1643 cm⁻¹ occurred due to the asymmetric stretching relaxation of the B-O band of trigonal BO_3 units [22]. The deconvoluted IR bands along with their assignment are given in **Table 3**. It is observed that the doping of Co and Mo to the prepared glass network cause a small shift with an irregular pattern in the absorption bands.

3.4. Optical Properties

The optical absorption spectra of the studied glasses are illustrated in **Figure 3**. No bands appeared in the Co and Mo free sample. The Mo and Co doped glasses were iteratively deconvoluted as shown in **Figure 4** to extensively explore the valence states of Mo and Co ions. The sample that contains 1 mol% of Mo without any Co ion content not included in this study because it was found to be opaque and could not measure its optical properties.

Table 3: Summary of FTIR spectral band positions of the investigated glasses

Sample No.	O=P-O	B-O-B	P-O-P, $P_2O_7^{4-}$, & BO_4	P-O, PO_3 , & BO_4	PO_2 & BO_3	B-O-B in $[BO_3]$ triangles	B-O	
S0	532	700	987	1095	1265	1403	1527	1643
S1	516	694	987	1126	1265	1403	1535	1650
S2	524	701	987	1110	1272	1403	1527	1650
S3	532	701	995	1095	1265	1403	1527	1643
S4	532	701	987	1103	1257	1403	1527	1643
S5	532	701	995	1118	1272	1403	1527	1643

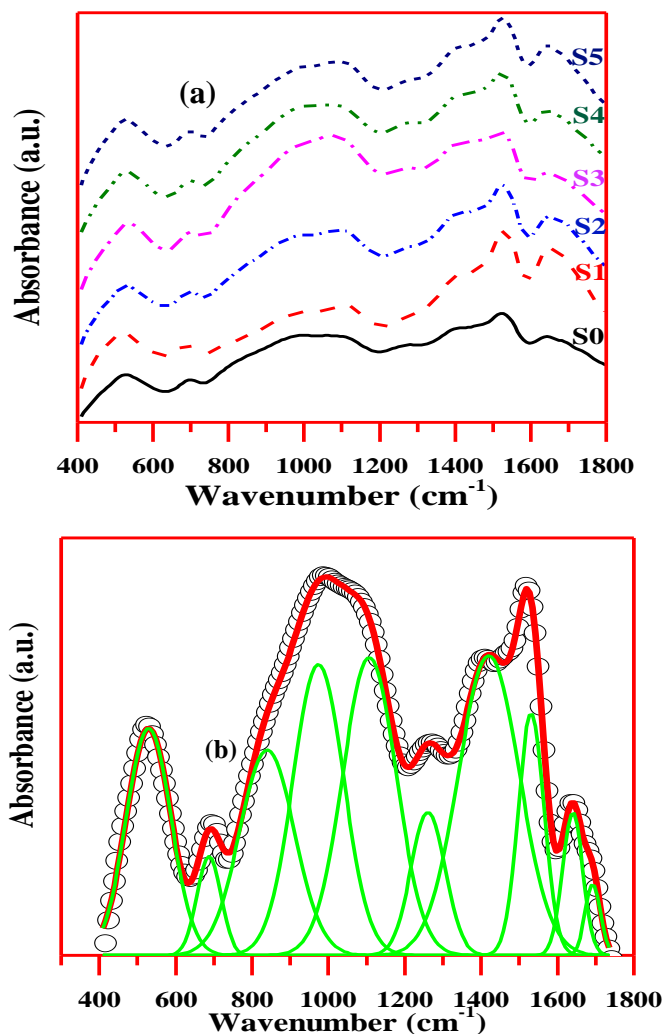


Fig 2: a) FTIR spectra and b) Representative deconvolution spectrum of the investigated glasses

In 1 mol% of Co, three absorption bands are observed at 523, 582, and 632 nm. The band centred at 523 nm was identified as being due to ${}^4T_{1g}(F) \rightarrow {}^2T_{1g}(H)$ octahedral transition of Co^{2+} . The band centred at 582 nm was attributed to the spin- and electric-dipole-allowed ${}^4A_{2g}({}^4F) \rightarrow {}^4T_{1g}({}^4P)$ transitions of tetrahedral coordinated of Co^{2+} ions [23-24]. The band at 632 nm was assigned to ${}^5T_{2g} \rightarrow {}^5E_g$ octahedral transition of Co^{3+} ions. At 0.4 mol% of Mo ion, two additional bands are observed located at 478 nm and 649 nm. The band located at 478 nm is related to the Mo^{3+} state, while that located at 649 nm corresponding to the Mo^{5+} ion. The low intensity that generated at ~ 795 nm in 0.6 mol % of Mo may be related to the excitation of $Mo^{5+}(4d^1)$ ion [8-9]. The generation of the band 795 nm at 0.6 mol % of Mo only is a strange result.

The optical band gap values (E_g) were evaluated using the observed absorption edges. It is customary to plot of $(ah\nu^{1/2})$ versus energy ($h\nu$) to find the optical energy band gaps E_g using Davis and Mott relation from the linear extrapolation to the zero ordinate.

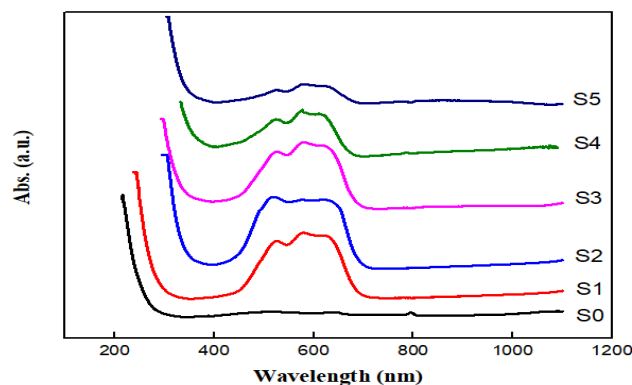


Fig 3: Optical absorption spectra of the investigated glasses

Urbach energy (ΔE) was obtained from the reciprocal slope of the graph of absorption coefficient logarithm ($\ln\alpha$), versus the photon energy ($h\nu$) [25-26]. The variation in optical band gap (E_g) and Urbach energy (ΔE) values for different samples are shown in Figure 5. It has been observed that the variation of the gap energy and Urbach energy is non-monotonic with the cobalt and molybdenum doping level. The formation of NBOs and localized states in the energy gap as well as the electronic shell of O^{2-} ion is affected by the highly polarizing action of modifying cation may cause the fluctuation in E_g .

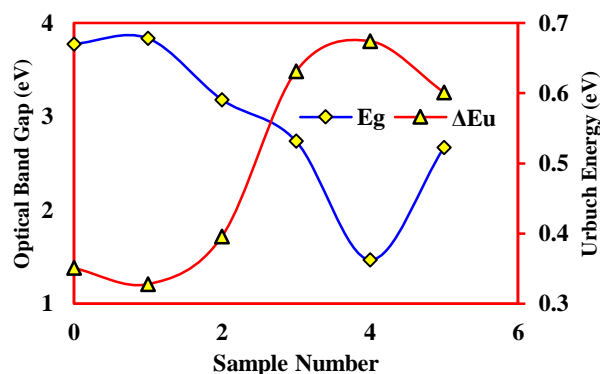


Fig 5: Variation of optical band gap and Urbach energy

The refractive index (n), Electronic polarizability of oxide ions [$\alpha_0^{2-}(n)$], experimental dielectric constant (ϵ), metallization [$M(n)$], and experimental optical basicity ($\Lambda_{Exp.}$) are deduced using the following formulae [23-24]:

$$\frac{n^2 - 1}{n^2 + 2} = 1 - \sqrt{E_g/20}$$

$$\alpha_0^{2-}(n) = \frac{[R_m - \sum \alpha_i]}{N_{O^{2-}}}$$

$$M(n) = 1 - \frac{\rho R_m}{M}$$

$$\Lambda_{Exp.}(n) = 1.67 \left(1 - \frac{1}{\alpha_0^{2-}(n)} \right)$$

where R_m is the molar fraction, α_i cation polarizability, $N_{O^{2-}}$ is the number of oxide ions in the chemical formula and M is the molar mass of the prepared glasses.

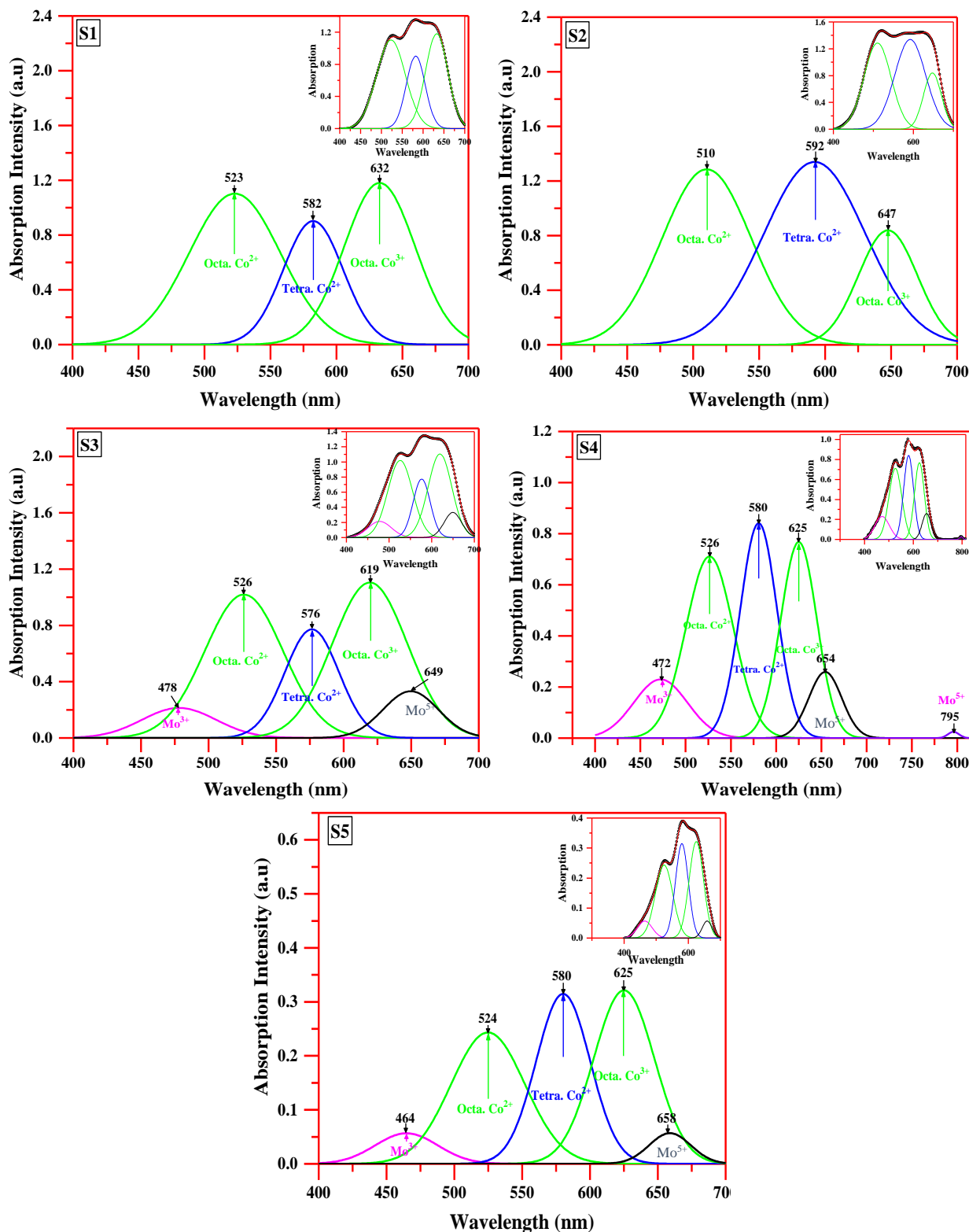


Fig 4: Deconvolution of the obtained optical absorption for the studied glasses

The estimated parameters are tabulated in **Table 2**. The fluctuation in the electronic polarizability and refractive index (n) may be attributed to the non-bridging oxygen formed in the glass network.

The NBOs create more ionic bonds, which manifest themselves in a larger polarizability over the covalent bonds of BOs, providing a higher refractive index value. The electronic polarizability and metallization have an opposite trend which attributed to break down of borate & phosphate

bonds to create non-bridging oxygen atoms. The metallization values of the present glasses are found to be less than one, which means that the width of both valence and conduction bands becomes large. Hence, the present glass system should exhibit an insulating nature. The variation of optical basicity of glasses with the increase of MoO₃ content could be attributed to the variation in negative charges on the oxygen atoms and, thus, increases in covalency force in the cation-oxygen bonding.

Conclusions

Combined structural and optical spectral measurements were carried out for zinc-sodium-borophosphate glasses containing MoO₃ and CoO. The results of density and its deduced parameters showed that compactness and packing of the glass network. FTIR absorption spectra of the undoped glass reveal characteristic vibrational modes due to borate and phosphate groups. The addition of CoO and MoO₃ within the doping level causes minor variations and the main characteristic network building units remain unchanged. The optical spectrum of the undoped cobalt and molybdenum glass showed no absorption bands. Spectral data indicate that divalent cobalt ions are mainly present in the octahedral coordination states and a small concentration of tetrahedral state. On the other hand, molybdenum ion exists in trivalent Mo³⁺ and pentavalent Mo⁵⁺ oxidation states. The fluctuation in many calculated structural and optical parameters indicates that the complex changes in the glass network due to the variation in ration of two transition metal in the complicated borophosphate glass. The present glasses have a selective property of a certain wavelengths in visible region which, opens up multiple horizons for it to be used in many optical applications

Conflicts of interest

The authors declare no conflicts of interest.

Funding

The authors did not receive support from any organization for the submitted work.

Authors' contributions

The article point was proposed by **M. A. Farag and Aly Saeed**. All authors contributed to the study conception and design. Samples preparation, data collection and analysis were performed by all authors. The manuscript was written and revised by all authors.

References

- 1- Cynthia Sundararaj, Suresh Sagadevan, *Materials Research*, Vol. 21, No. 1, PP.1-7 (2018).
- 2- Aly Saeed, Y. H. Elbashar, and S. U. El Kameesy, *Research Journal of Pharmaceutical, Biological and Chemical Sciences*, Vol. 6, No. 4, PP. 1390-1397 (2015).
- 3- Y. H. Elbashar, Aly Saeed and S. S. Moslem, *Nonlinear Optics and Quantum Optics*, Vol. 0, PP. 1–8 (2016).
- 4- L. Koudelka and P. Mořner, *Materials Letters*, Vol. 42, PP. 194–199 (2000).
- 5- Christian Hermansen, Randall E. Youngman, John Wang, and Yuanzheng Yue, *The Journal of Chemical Physics*, Vol. 142, PP. 1-13 (2015).
- 6- A. M. Abdelghany, F. H. ElBatal, M. A. Azooz, M. A. Ouis, H. A. ElBatal, *Spectrochimica Acta Part A: Molecular and Biomolecular Spectroscopy*, Vol.98, PP.148–155 (2012).
- 7- H. Elhaes, M. Attallah, Y. Elbashar, M. El-Okr, M. Ibrahim, *Physica B*, Vol.449, PP.251–254 (2014).
- 8- A. Agarwa, S. Khasa, V.P. Seth, S. Sanghi, M. Arora, *Journal of Molecular Structure*, Vol. 1060, PP.182–190 (2014).
- 9- A.M. El-Batal, Aly Saeed, N. Hendawy, M.M. El-Okr, M.K. El-Mansy, *Journal of Non-Crystalline Solids*, Vol. 559, 120678, (2021).
- 10- P. Petkova, M.T. Soltani, S. Petkov and V. Nedkov, *Acta Physica Polonica A*, Vol. 121, No.1, PP.152-154 (2012).
- 11- G. Lakshminarayana, S. Buddhudu, *Spectrochimica Acta Part A*, Vol. 63, PP. 295–304 (2006).
- 12- H. Elhaes, M. Attallah, Y. Elbashar, A.Al-Alousi, M. El-Okr, and M. Ibrahim, *Journal of Computational and Theoretical Nanoscience*, Vol. 11, PP. 1–6, 2014.
- 13- Y. H. Elbashar, *Silicon*, Vol. 9, No. 5, PP. 711–715 (2017).
- 14- A. Saeed, Y. H. Elbashar, R. M. El shazly, *Optical and Quantum Electronics*, Vol.48, No.1, PP.1-10 (2016).
- 15- M.D.Thombare, R.V.Joat, D.B. Thombre L, *International Journal of Engineering Science and Computing*, Vol. 6, No. 7, PP. 8482-8487 (2016).
- 16- A. Saeed, Y. H. Elbashar and S. U. El Kameesy, *Silicon*, Vol. 10, PP.185–189 (2018).
- 17- Simranpreet Kaur, Gurinder Pal Singh, Parvinder Kaur, D.P. Singh, *J. Lumin.* Vol. 143, PP. 31–37 (2013).
- 18- Chandkiram Gautam, Avadhesh Kumar Yadav, and Arbind Kumar Singh, *International Scholarly Research Network*, Volume 2012, PP. 1-17 (2012).
- 19- R. Lucacel Ciceo, M. Todea, R. Dudric, A. Buhai, V. Simon, *Journal of Non-Crystalline Solids*, Vol. 481, PP. 562-567 (2018).
- 20- A.M. Abdelghany, F.H. ElBatal, H.A. ElBatal, F.M. EzzElDin, *Journal of Molecular Structure*, Vol.1074, PP.503–510 (2014).
- 21- Ramesh Bodaa and, Md.Shareefuddin, M.N Charya, R.Sayanna, *Materials Today: Proceedings*, Vol. 3, PP.1914–1922 (2016).
- 22- V. Dimitrov, T. Komatsu, *Journal of the University of Chemical Technology and Metallurgy*, Vol. 45, No. 3, PP. 219-250 (2010).
- 23- M. Farouk, *Optik*, Vol. 140, PP. 186-196 (2017).
- 24- G. Krishna Kumari, Sk. Muntaz Begum, Ch. Rama Krishna, D.V. Sathish, P.N. Murthy, P.S. Rao, R.V.S.S.N. Ravikumar, *Materials Research Bulletin*, Vol. 47, No. 9, PP. 2646-2654 (2012).
- 25- T. Raghavendra Rao, Ch. Rama Krishna, Ch. Venkata Reddy, U.S. Udayachandran Thampy, Y.P. Reddy, P.S. Rao, R.V.S.S.N. Ravikumar, *Spectrochimica Acta Part A: Molecular and Biomolecular Spectroscopy*, Vol. 79, No. 5, PP. 1116-1122 (2011).
- 26- M. Farouk, A. Samir, A. Ibrahim, M. A. Farag, A. Solieman, *Raman, Applied Physics A*, Vol 126:696 (2020)
- 27- A. A. Elbakey, M. A. Farag, M. El-Okr, T. Y. Elrasasi, M. K. El-Mansy, *Egypt.J.Chem.* Vol. 63, No. 5. pp. 1955 - 1964 (2020)
- 28- Constantin I. Andronache, Dania Racolta, *AIP Conf. Proc.* 1634, PP. 115-119 (2014).